

# Pairing Correlations in Odd-Mass Carbon Isotopes and in $^{11}\text{Be}$

A.R. Samana<sup>1,2</sup>, T. Tarutina<sup>1</sup>, F. Krmpotić<sup>1,2,3</sup>, and M.S. Hussein<sup>1</sup>

<sup>1</sup>*Departamento de Física Matemática,*

*Instituto de Física da Universidade de São Paulo,*

*Caixa Postal 66318, 05315-970 São Paulo, SP, Brazil*

<sup>2</sup>*Instituto de Física La Plata, CONICET, 1900 La Plata, Argentina and*

<sup>3</sup>*Facultad de Ciencias Astronómicas y Geofísicas,*

*Universidad Nacional de La Plata, 1900 La Plata, Argentina*

(Dated: February 9, 2020)

## Abstract

In this paper we present an exploratory study of structure of the odd-mass carbon isotopes  $^{15}\text{C}$ ,  $^{17}\text{C}$  and  $^{19}\text{C}$ , using the BCS and the projected BCS (PBCS) models to assess the importance of pairing correlations in these light nuclei. Further, we consider the structure of  $^{13}\text{C}$  and  $^{11}\text{Be}$  using the quasiparticle-rotor model to better understand the origin of spin and parity of the levels and the degree of deformation of the corresponding cores. The quasiparticle-vibrator model is also employed as an alternative model. Comparison of our results with several recent papers on the same subject is also presented. We have shown that the inclusion of the pairing interaction and of the concomitant Pauli principle is imperative for a realistic description of heavy odd-mass carbon isotopes and in the core-coupling models for  $^{13}\text{C}$  and  $^{11}\text{Be}$ . The important role played by the particle number conservation in relatively light and/or exotic nuclei has been confirmed as well.

## I. INTRODUCTION

It has been known for a long time that the structure of the nucleus depends significantly on their superfluid nature. In fact, pairing constitutes the main part of the residual interaction beyond the Hartree-Fock (HF) approximation and has a strong influence on most low-energy properties of the system [1]. This encompasses masses, separation energies, deformation, individual excitation spectra and collective excitation modes such as rotation or vibration. The role of pairing correlations is particularly emphasised when going toward the neutron drip-line because of the proximity of the Fermi surface to the single-particle continuum. Indeed, the scattering of virtual pairs into the continuum gives rise to a variety of new phenomena in ground and excited states of nuclei [2].

Despite its major role, our knowledge of the pairing force and of the nature of pairing correlations in nuclei is rather poor. The importance of resolving the range of the interaction, the nature and characteristics of its density dependence have to be clarified. In addition, the influence of the restoration of particle-number and pairing vibrations in even and odd nuclei still has to be characterised through systematic calculations.

Many experimental and theoretical investigations for over two decades were concentrated upon study of light nuclei near neutron drip line (see references in recent reviews [3, 4]). The unusual properties of these nuclei have been a challenge for conventional nuclear structure models. In Refs.[5, 6] it was shown that the increase in pairing correlations and the shallow single-particle potentials for nuclei close to the drip-lines may result in a more uniformly spaced spectrum of single particle states. The famous example of the  $1s_{1/2}$  intruder state in  $^{11}\text{Be}$  suggests that the  $N = 8$  magic number is disappearing. The experiment on inelastic proton scattering of  $^{12}\text{Be}$  in inverse kinematics [7] provides another indication of the  $N = 8$  shell melting. A more direct observation of the disappearance of magicity in  $^{12}\text{Be}$  was obtained using the one-neutron knockout reactions of  $^{12}\text{Be}$  on  $^{9}\text{Be}$  target measured at MSU [8].

There is evidence for a new neutron magic number with  $N = 16$ . In Ref. [9] the analysis of neutron separation energies and interaction cross sections for neutron-rich nuclei in the  $p$  and  $sd$  regions shows evidence for this new magic number. There are other studies that support this assignment (see Refs. [10, 11]).

A series of interesting works appeared in the literature recently which study the pair

correlation in spherical and deformed nuclei near the drip line, using a simplified HFB model in coordinate representation with the correct asymptotic boundary conditions. In analysing the effects of continuum coupling Hamamoto and Mottelson [12] found that for small binding energies the occupation probability decreases considerably for neutrons with low orbital momentum. In particular, they pointed out [13] that the effective pair gap was much reduced for the weakly bound neutrons in  $s_{1/2}$  state compared with that of neutrons with larger orbital momentum. In the presence of pair correlations, the large rms radius was obtained for neutrons close to the Fermi level, thus favouring the halo formation. Interestingly, in Ref. [14] the authors conclude that pair correlations prevent the rms radii from becoming infinitely large. In Ref. [15] the dependence of effective pair gap on weakly bound neutron orbits was studied in the same model of Refs. [12, 13] and was found to be very small for  $\frac{1}{2}^+$  states.

All above suggests that the pairing correlations play a relevant role in the structure of light exotic nuclei. However, the parity inversion in  $^{11}\text{Be}$  is frequently attributed only to the quadrupole core excitation effects. That is, the fact that in this nucleus the ground state is a  $\frac{1}{2}^+$  state and not a  $\frac{1}{2}^-$  state, as dictates the spherical shell model, is described within the simple particle-vibration coupling model (PVM) [16, 17], or particle-rotor coupling model (PRM) [18, 19, 20, 21], where the correlations among the valence particles, coming from the residual interaction, are totally neglected. We know, however, that, while the positive parity states in  $^{11}\text{Be}$  can be accounted for fairly well in the weak coupling model [20], the low-lying negative parity states cannot be described reliably without including the pairing correlations [22]. The same statement is also valid for the  $^{13}\text{C}$  nucleus. In fact, recently it has been found [23] that the low-lying energy spectra in the last nucleus can be described quite well in the context of the number projected BCS (PBCS) approximation for the pairing force among the valence neutrons [24]. More precisely, in Ref. [23] it was shown that the projection procedure is very important in light nuclei, where the number of neutrons is small.

The aim of the present work is twofold. Firstly, we would like to inquire to which extent the main feature of heavy carbon isotopes  $^{15}\text{C}$ ,  $^{17}\text{C}$ , and  $^{19}\text{C}$  can be interpreted in the framework of the PBCS model, using as a building block the results obtained in Ref. [23] for the stable carbon isotope  $^{13}\text{C}$ . One should keep in mind that as the number of neutrons increases, in going from  $^{13}\text{C}$  to  $^{19}\text{C}$ , the nuclei become more and more exotic. In fact, the recent extensive studies of the heavy carbon isotopes,  $^{17}\text{C}$  and  $^{19}\text{C}$ , suggest that

they are candidates to possess neutron halo, especially the last one. Secondly, we discuss the interplay of the single-particle and collective degrees of freedom in  $^{13}\text{C}$  and  $^{11}\text{Be}$ . Our choice of  $^{11}\text{Be}$  resides in the fact that it is considered a reasonably well formed one neutron halo that exhibits, among other things, parity inversion. We further generalize previous works [16, 17, 18, 19, 20, 21] by considering the modification in the single-particle degree of freedom implied by the pairing correlations [25, 26, 27, 28]. Therefore, we will discuss the structure of these two nuclei in the framework of the quasiparticle-rotor model (QPRM) and the quasiparticle-vibrator model (QPVM). The corresponding models with the particle number projection included will be labelled, respectively, as PQPRM and PQPVM.

This paper is organised as follows: In the next section (section II) we describe particle-rotor model and introduce the quasiparticle-rotor model. In section III we present the results of structure calculations for carbon isotopes, that is the ground and excited states energies and the structure of the wave functions. Finally, section IV contains summary and conclusions of this work.

## II. PAIRING DESCRIPTION OF ODD-MASS CARBON ISOTOPES

The definitions of particle and hole states  $E_j^{(\pm)}$  in the BCS and PBCS approximations are listed in Table I, where

$$E_j = (\bar{e}_j^2 + \Delta_j^2)^{1/2}, \quad (2.1)$$

are the usual BCS quasiparticle energies, which depend on the renormalised single-particle energies (s.p.e.)

$$\bar{e}_j = e_j - l + \sum_{j'} \frac{(2j'+1)^{1/2}}{(2j+1)^{1/2}} v_{j'}^2 F(jjj'j'; 0), \quad (2.2)$$

and on the pairing gap

$$\Delta_j = -\frac{1}{2} \sum_{j'} \frac{(2j'+1)^{1/2}}{(2j+1)^{1/2}} u_{j'} v_{j'} G(jjj'j'; 0). \quad (2.3)$$

$e_j$  are the bare s.p.e..

The PBCS energies read

$$\varepsilon_j^N = \frac{R_0^N(j) + R_{11}^N(jj)}{I^N(j)} - \frac{R_0^N}{I^N}. \quad (2.4)$$

TABLE I: Definitions of particle ( $E_j^{(+)}$ ), and hole ( $E_j^{(-)}$ ) energies in the BCS and PBCS approximations. In both cases,  $E_j^{(+)}$  can be either negative or positive, while  $E_j^{(-)}$  are always negative. The BCS quasiparticle energies  $E_j$ , defined in (2.1), are positive, and the corresponding chemical potential  $\lambda$  is negative. The PBCS quasiparticle energies  $\varepsilon_j^N$  are defined in (2.4).

Model	$E_j^{(+)}$	$E_j^{(-)}$
BCS	$\lambda + E_j$	$\lambda - E_j$
PBCS	$\varepsilon_j^N$	$-\varepsilon_j^{N-2}$

The quantities  $R^N$  and  $I^N$ , where  $N$  is the neutron number, are defined in Ref. [24]. In the present case  $N = 6$ .

The BCS and PBCS predictions for the spectroscopic factors will be also discussed. Within the PBCS approximation they are given by [24, 29]:

$$S_u(j) = u_j^2 \frac{I^N(j)}{I^N}, \quad (2.5)$$

for the stripping reactions on even targets and for pick up reactions on odd targets, and by

$$S_v(j) = (2j+1)v_j^2 \frac{I^{N-2}(j)}{I^N}, \quad (2.6)$$

for the stripping reactions on odd targets and for pick up reactions on even targets. The plain BCS results are recovered by making all the  $I$ -factors equal to unity.

The BCS and PBCS calculations shown here were done in the same way as in the previous work [23]. That is, for the residual interaction we adopted the delta force,

$$V = -4\pi v^{pair} \delta(r) \text{ MeV-fm}^3, \quad (2.7)$$

and the configuration space includes the neutron orbital with  $j \equiv nlj = (1s_{1/2}, 1p_{3/2}, 1p_{1/2}, 1d_{5/2}, 2s_{1/2}, 1d_{3/2}, 1f_{7/2}, 1f_{5/2})$ . The radial wave functions were approximated with that of the harmonic oscillator (HO) with the length parameter  $b = 1.67$  fm, which corresponds to the estimate  $\hbar\omega = 45A^{-1/3} - 25A^{-2/3}$  MeV for the oscillator energy. Moreover, the bare s.p.e.  $e_j$ , as well as the value of the singlet pairing strength  $v^{pair}$ , were fixed by adjusting the experimental energies to the calculated ones, through a  $\chi^2$  search,

TABLE II: The experimental energies  $E_j^{exp}$  used in the fitting procedure, and the resulting single-particle energies  $e_j$ , and the pairing strength  $v_s^{pair}$  within the BCS and PBCS. The energies are given in units of MeV, and  $v_s^{pair}$  is dimensionless.

Shell	$E_j^{exp}$	$e_j(BCS)$	$e_j(PBCS)$
$1s_{1/2}$		−23.58	−22.37
$1p_{3/2}$	−18.72	−7.80	−7.24
$1p_{1/2}$	−4.94	−2.07	−1.51
$1d_{5/2}$	−1.09	2.12	2.16
$2s_{1/2}$	−1.85	2.70	2.68
$1d_{3/2}$	2.72	6.24	6.26
$1f_{7/2}$	5.81	8.14	8.17
$2p_{3/2}$	7.17	11.49	11.47
$2p_{1/2}$		17.30	17.32
$1f_{5/2}$		19.18	19.21
$v_s^{pair}$		23.16	23.92

assuming that: a) the ground state  $3/2^-$  in  $^{11}\text{C}$  is a pure  $1p_{3/2}$  hole-state  $E_{1p_{3/2}}^{(-)}$ , and b) the lowest  $1/2^-, 5/2^+, 1/2^+, 3/2^+, 7/2^-$ , and  $3/2^-$  states in  $^{13}\text{C}$  are pure particle-states  $E_j^{(+)}$  with  $j = (1p_{1/2}, 1d_{5/2}, 2s_{1/2}, 1d_{3/2}, 1f_{7/2}, 2p_{3/2})$ . The s.p.e. of the faraway orbital  $1s_{1/2}$ ,  $2p_{1/2}$  and  $1f_{5/2}$  are approximated by that of a HO with standard parametrisation [30]. The experimental energies  $E_j^{exp}$  used in the fitting procedure, and the resulting S.p.e.  $e_j$ , and pairing strength  $v_s^{pair}$  are listed in Table II. The relationship between the s.p.e. and the corresponding quasiparticle energies are illustrated in Fig. 1. The major difference between the BCS and the PBCS results appears in the hole states  $1s_{1/2}$  and  $1p_{3/2}$ .

After fixing the parameterisations ( $e_j$  and  $v_s^{pair}$ ) in  $^{13}\text{C}$ , we evaluate the low-lying energy spectra for the remaining odd-mass carbon isotopes, by modifying only the number of neutrons. In another words, we solve the BCS and PBCS gap equations with the parameters listed in Table II and the number of particles  $N = 8, 10$ , and  $12$  for  $^{15}\text{C}$ ,  $^{17}\text{C}$  and  $^{19}\text{C}$ , respectively. The results for the energy spectra and the spectroscopic factors are shown in

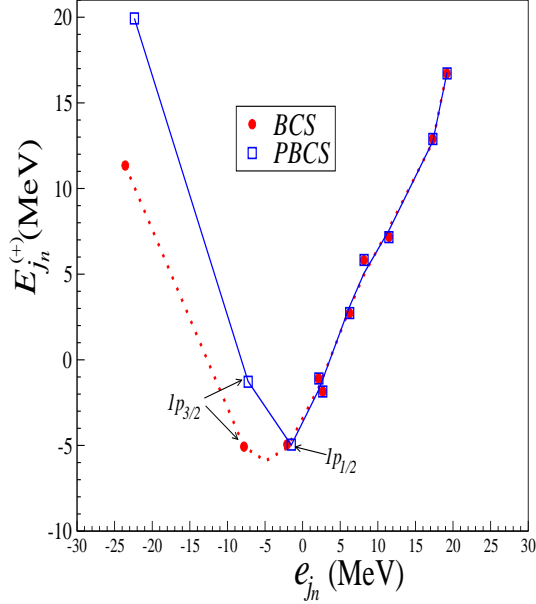


FIG. 1: Relationship between the single-particle and the quasiparticle excitation energies for  $^{13}\text{C}$ . The states are ordered as  $1s_{1/2}$ ,  $1p_{3/2}$ ,  $1p_{1/2}$ ,  $2s_{1/2}$ ,  $1d_{3/2}$ ,  $1f_{7/2}$ ,  $2p_{3/2}$ ,  $2p_{1/2}$ , and  $1f_{7/2}$ , and the energies are indicated by filled circles (BCS) and unfilled squares (PBCS).

Figs. 2 and 3, respectively. One immediately see the pairing interaction accounts for the main nuclear structure features of these nuclei as they become more and more exotic when the mass number  $A$  is increased. In particular, the decrease of the separation energies in going from  $^{13}\text{C}$  to  $^{19}\text{C}$  is fairly well reproduced.

The experimentally observed spin ordering  $1/2^+, 5/2^+, 3/2^+$  of the lowest three states in  $^{15}\text{C}$ , as well as energy of the first  $3/2^-$ , are also reproduced within the PBCS. In both cases the number projection plays a quite significant role. The states  $5/2^-$  and  $1/2^-$  at 4.22 MeV and 4.66 MeV are very likely seniority-three states which are not contained in our configuration space. The inversion between the  $5/2^+$  and  $1/2^+$  states in  $^{15}\text{C}$  is seldom considered to be a “exotic” feature of this nucleus [33, 34]. That is, it is attributed to the halo formation, which makes the lowest angular momentum to gain energy by extending its wave function. In our model this apparent “anomaly” is just a consequence of the pairing interaction and it already takes place in  $^{13}\text{C}$ , as can be seen from Table II and Fig. 2:  $e_{1d_{5/2}} < e_{2s_{1/2}}$  while  $E_{1d_{5/2}}^{(+)} > E_{2s_{1/2}}^{(+)}$ .

The separation energy of the last neutron in  $^{17}\text{C}$  is  $S_n = 729 \pm 18$  keV [35], while the shell model calculation [36] predicts a  $J^\pi = 3/2^+$  ground state. This prediction has

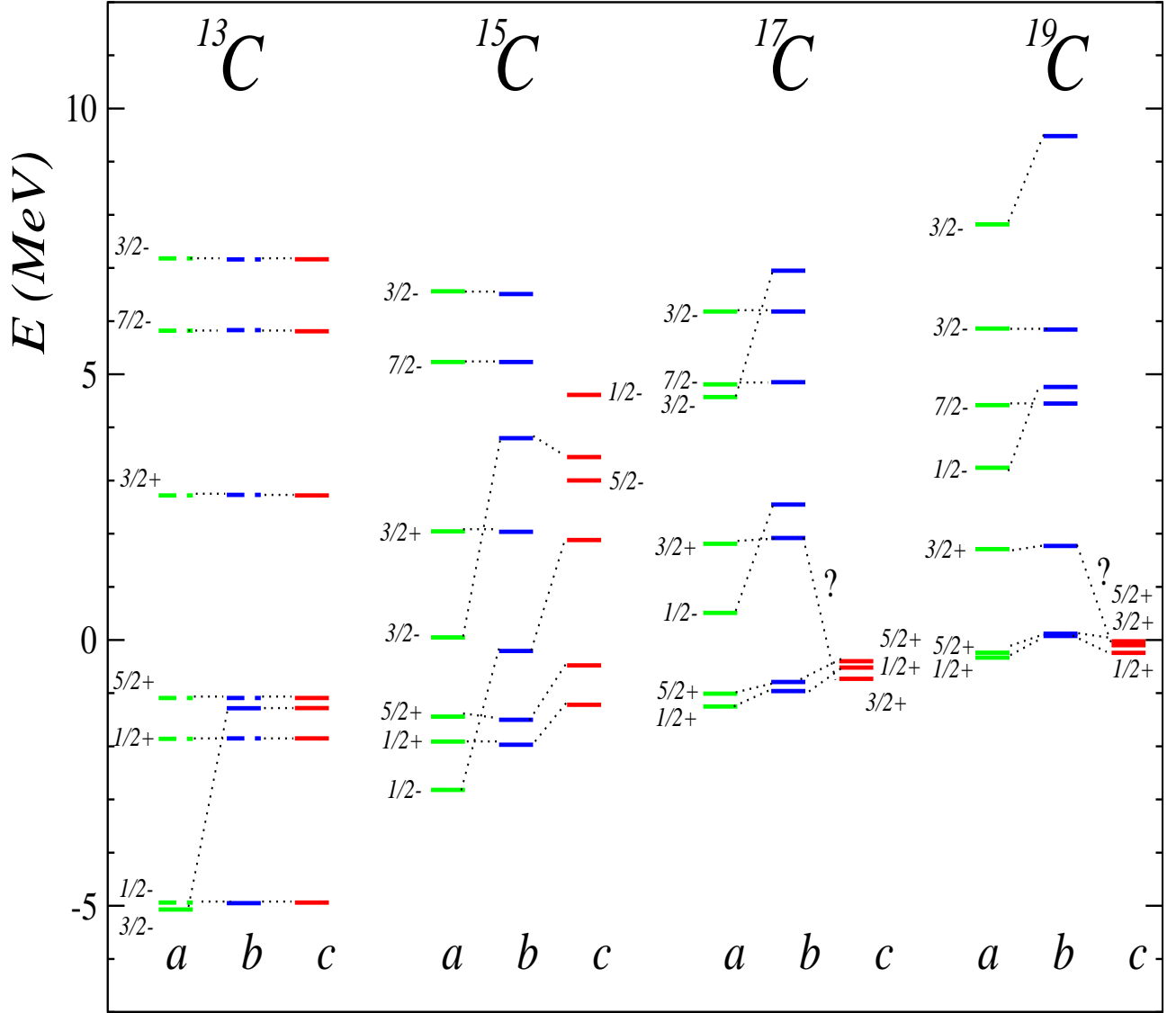


FIG. 2: Comparison between the calculated BCS, PBCS and measured level schemes for odd mass carbon isotopes: a) BCS, b) PBCS, and c) experiments: from Ref. [31] for  $^{13}\text{C}$ ,  $^{15}\text{C}$ , and Ref. [32] for  $^{17}\text{C}$  and  $^{19}\text{C}$ .

been confirmed later on by the single-neutron knockout reaction measurements done by Maddalena *et al.* [37], which strongly indicates such an assignment instead of the naively expected option  $J^\pi = 5/2^+$  arising from the seniority-one state  $|(1d_{5/2})^3 J^\pi = 5/2^+\rangle$ . A simple explanation for this experimental result could be found in the so called  $J = j - 1$  anomaly discussed by Bohr and Mottelson [38]. In fact, since the work of Kurath [39] we know that for  $(j)^3$  configurations with  $j \geq 5/2$ , the  $J = j - 1$  state can occur below the

$J = j$  state for sufficiently long range forces. The same effect can be achieved as well in the Alaga model, as a consequence of the coupling of the three-particle cluster ( $j$ )<sup>3</sup> to the quadrupole vibrational field. For instance, in this way has been explained the low-lying positive parity states in odd-mass silver isotopes [40, 41]. The simple model discussed here does not contain seniority-three states and therefore it is unable to account for the  $3/2^+$  ground state spin. However, as seen from the Fig. 2, it predicts that the first two excited states are  $1/2^+$  and  $5/2^+$  (in this order), which is consistent with the recent measurement done by Elekes *et al.* [32].

Special attention was given to the neutron-rich carbon isotope  $^{19}\text{C}$  to establish whether it has one-neutron-halo as suggested in Refs. [21, 42]. On the basis of measurements of different observables, associated with the neutron-removal reaction [37, 43, 44], there seems to be consensus that the spin and parity of its ground state is  $J^\pi = 1/2^+$ . Contrarily, there is a strong discrepancy in the literature regarding the separation energy of  $^{19}\text{C}$ . The tabulated values go from  $S_n = 160 \pm 95$  keV in 1993-1997 [45] to  $S_n = 580 \pm 90$  keV in 2003 [46]. The experiments using time-of-flight techniques suggest small separation energy, that is, weighted average yields  $S_n = 242 \pm 95$  keV [42]. The Coulomb dissociation of  $^{19}\text{C}$  was studied by Nakamura in [43], and the analysis of angular distributions of breakup products suggests the value  $S_n = 0.53 \pm 0.13$  MeV. Using this value in the simple cluster model calculation of the dipole strength gives good agreement with the data. On the other hand, more recent experiment of Maddalena *et al.* [37] on nuclear breakup of  $^{19}\text{C}$  yields  $S_n = 0.65 \pm 0.15$  MeV and  $0.8 \pm 0.3$  MeV. In the present calculation we correctly reproduce the spin and parity of the ground state. For its energy we obtain  $-0.33$  MeV in the BCS and  $0.12$  MeV in the PBCS. Both results are in fair agreement with the values reported in Refs. [42, 45]. Two excited states at energies of  $197(6)$  keV and  $269(8)$  keV were reported in a recent study of the  $\gamma$ -ray spectra [32]. The suggested spins and parities are  $3/2^+$  and  $5/2^+$ , and seen from Fig. 2 we reproduce these states but in the inverted order.

The BCS and PBCS one-particle reaction spectroscopic factors for the lowest  $J^\pi = 1/2^-, 3/2^-, 1/2^+$  and  $5/2^+$  states in odd-mass carbon isotopes are shown in Fig. 3, as a function of the mass number  $A$ . They are quite similar to each other, and, except for  $^{13}\text{C}$ , they also agree fairly well with the experimental data which are displayed in the same figure. This concordance clearly implies that in  $^{15}\text{C}$ -  $^{19}\text{C}$  nuclei the states  $J^\pi = 1/2^-, 1/2^+$  and  $5/2^+$  are basically seniority-one states. Contrarily, the contribution of seniority-three

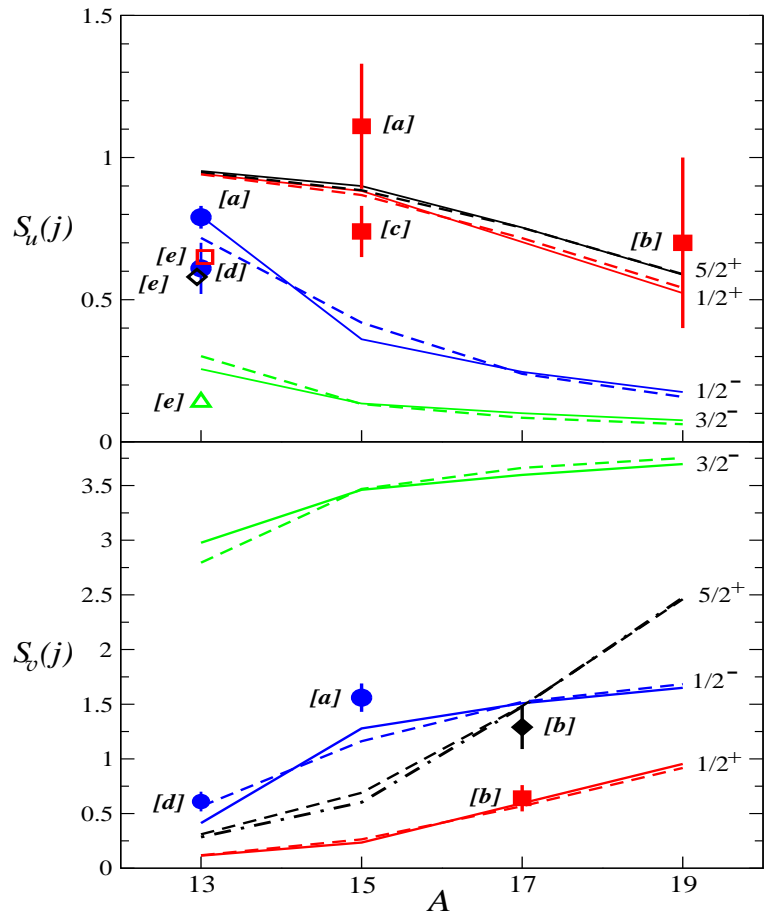


FIG. 3: (Color online) One-particle reaction spectroscopic factors as a function of the mass number  $A$ . Upper panel:  $S_u(j)$ , for stripping on even parent and pick-up/ knock-out on odd parent. Lower panel:  $S_v(j)$ , for pick-up/knock-out on even parent and stripping on odd parent. The dashed and solid lines correspond, respectively, to the BCS and PBCS predictions. The experimental values for the lowest  $J^\pi = 1/2^-, 3/2^-, 1/2^+$  and  $5/2^+$  states are indicated, respectively, with circles, triangles, squares, and diamonds. The data were by recompiled from Refs.: [47]<sup>[a]</sup>, [37, 48]<sup>[b]</sup>, [48, 49]<sup>[c]</sup>, [50]<sup>[d]</sup> and [51]<sup>[e]</sup>.

states, and/or of the collective degrees of freedom seems to be quite relevant in  $^{13}\text{C}$ . The latter will be discussed in the next section.

### III. $^{13}\text{C}$ AND $^{11}\text{BE}$ WITHIN QUASIPARTICLE-CORE MODEL

#### A. Quasiparticle-Rotor Model

As usually done [38], the rotor here is assumed to posses axial symmetry, and its angular momentum is denoted by  $\mathbf{R}$  with the component  $R_3 = 0$  with respect to the symmetry axis.

The corresponding Hamiltonian is

$$H_{\text{rot}} = \frac{\hbar^2(R_1^2 + R_2^2)}{2\mathcal{I}} = \frac{\hbar^2}{2\mathcal{I}}\mathbf{R}^2, \quad (3.1)$$

where  $\mathcal{I}$  stands for the moment of inertia, and the spectrum consists of the sequence  $R = 0, 2, 4, \dots$ .

The interaction between the rotor and the particle is described by a potential  $U(r, \theta')$ , depending on the variables of the particle in the body fixed coordinates, and the Hamiltonian for the coupled particle-core system is

$$H_{\text{par-rot}} = H_{\text{rot}} + T + U, \quad (3.2)$$

where  $T$  is the kinetic energy of the particle. The deformed potential is expanded in the form

$$U(r, \theta') \cong U_0(r) + H_{\text{int}} \quad (3.3)$$

where  $U_0(r) \equiv U(r, 0)$ , and  $H_{\text{int}}$  is the core-nucleon coupling Hamiltonian. We consider here the quadrupole deformation only, specified by the deformation parameter  $\beta$ . In this case

$$H_{\text{int}} = -\beta k(r)Y_{20}(\theta', 0); \quad k(r) \equiv r \frac{dU_0(r)}{dr}. \quad (3.4)$$

The Hamiltonian (3.2) can now be rewritten as

$$H_{\text{par-rot}} = H_{\text{rot}} + H_{\text{sp}} + H_{\text{int}}, \quad (3.5)$$

where  $H_{\text{sp}} = T + U_0$  is single-particle (shell-model) Hamiltonian, whose eigenvalues  $e_j$  are specified by the particle angular momentum  $\mathbf{j}$ , *i.e.*,

$$[T + U_0(r)]\varphi_j(\mathbf{r}) = e_j\varphi_j(\mathbf{r}). \quad (3.6)$$

The total angular momentum is

$$\mathbf{I} = \mathbf{j} + \mathbf{R}, \quad (3.7)$$

and the coupling between  $\mathbf{j}$  and  $\mathbf{R}$  is clearly put in evidence in the weak-coupling representation of the total wave function, which reads

$$|jR; IM\rangle = \sum_{M_R m} (jmRM_R|IM) |jm\rangle |RM_R\rangle, \quad (3.8)$$

where  $|RM_R\rangle$  is the rotor wave function.

The matrix elements of the Hamiltonian (3.5) are:

$$\begin{aligned} \langle j'R'; IM | H_{\text{p-rot}} | jR; IM \rangle &= \left[ \frac{\hbar^2 R(R+1)}{2\mathcal{I}} + \varepsilon_j \right] \delta_{RR'} \delta_{jj'} \\ &- \beta \langle j' | k | j \rangle (-)^{I-\frac{1}{2}} \sqrt{\frac{5(2j+1)(2j'+1)(2R+1)(2R'+1)}{4\pi}} \\ &\times \begin{pmatrix} j' & 2 & j \\ \frac{1}{2} & 0 & -\frac{1}{2} \end{pmatrix} \begin{pmatrix} R & 2 & R' \\ 0 & 0 & 0 \end{pmatrix} \begin{Bmatrix} I & R' & j' \\ 2 & j & R \end{Bmatrix}. \end{aligned} \quad (3.9)$$

The resulting eigenfunctions are of the form:

$$|I_n\rangle = \sum_{jR} C_{jR}^I |jR; I\rangle, \quad (3.10)$$

with energies  $\mathcal{E}_{I_n}$ .

We now incorporate the residual interaction,  $V_{\text{res}}$ , between nucleons moving in an over-all deformed potential, and the total Hamiltonian becomes:

$$H_{\text{qp-rot}} = H_{\text{p-rot}} + V_{\text{res}}. \quad (3.11)$$

After carrying out a Bogoliubov-Valatin canonical transformation from particle to quasi-particle operators [25, 26], one gets that, independently of the residual interaction that is used, the matrix elements of  $H_{\text{qp-rot}}$  for odd-mass systems continue being of the form (3.9), except for:

1. The band-head energies are modified as:

$$e_j \rightarrow E_j^{(+)}, \quad (3.12)$$

with  $E_j^{(+)}$  defined in Table I, and

2. The non-diagonal particle-core matrix elements are renormalised by the overlap factors:

$$F_{jj'}^{QP} = u_j u_{j'} - v_j v_{j'}. \quad (3.13)$$

in the QPRM, and

$$F_{jj'}^{PQP} = \frac{u_j u_{j'} I^N(jj') - v_j v_{j'} I^{N-2}(jj')}{[I^N(j) I^N(j')]^{1/2}}, \quad (3.14)$$

in the PQPRM.

When the collective degrees of freedom are included, the spectroscopic factors (2.5) and (2.6) become:

$$S_u(I) = S_u(j = I) \left( C_{j,R=0}^I \right)^2, \quad (3.15)$$

for the stripping reactions on even targets and for pick up reactions on odd targets, and by

$$S_v(I) = S_v(j = I) \left( C_{j,R=0}^I \right)^2, \quad (3.16)$$

for the stripping reactions on odd targets and for pick up reactions on even targets. Here we only consider the processes that involve the ground state of the even nucleus.

TABLE III: Wood-Saxon s.p.e.  $e_j$  for  $^{13}\text{C}$  and  $^{11}\text{Be}$  and the corresponding quasiparticle BCS and PBCS energies  $E_j^{(+)}$ , and the energies  $E(2^+) = 3\hbar^2/\mathcal{I}$  of the collective  $2^+$  state.. The energies are given in units of MeV, and the pairing strength is  $v_s^{pair} = 30$ .

Shell	$^{12}\text{C}$			$^{10}\text{Be}$		
	$e_j$	$E_j^{(+)}$		$e_j$	$E_j^{(+)}$	
		BCS	PBCS		BCS	PBCS
$1p_{3/2}$	-13.54	-9.5956	-7.109	-7.33	-3.5928	-1.8592
$1p_{1/2}$	-7.82	-10.4057	-12.209	-2.59	-3.9583	-5.4577
$1d_{5/2}$	0.82	-4.2699	-4.123	3.50	0.2640	0.2333
$2s_{1/2}$	-0.61	-3.4033	-3.303	0.30	-2.0479	-2.1316
$E(2^+)$			4.438			3.368

The PRM differs in several important aspects from the QPRM and PQPRM. First, as shown in Fig. 1, the BCS and PBCS energies  $E_j^{(+)}$  can be quite different from the s.p.e.  $e_j$ , not only in magnitude but also in sign. Second, the factors  $F_{jj'}$ , which are quite similar in BCS and PBCS, correctly take in account the Pauli principle and they can be considerably less than unity for states near the Fermi level, diminishing in this way their coupling to the core excited states quite a lot. In addition, the particle-like states do not couple to the hole-like states, and if the particle-core coupling is attractive (repulsive) for a particle-like state  $j$ , it is repulsive (attractive) for a hole-like state with same quantum numbers  $j$ .

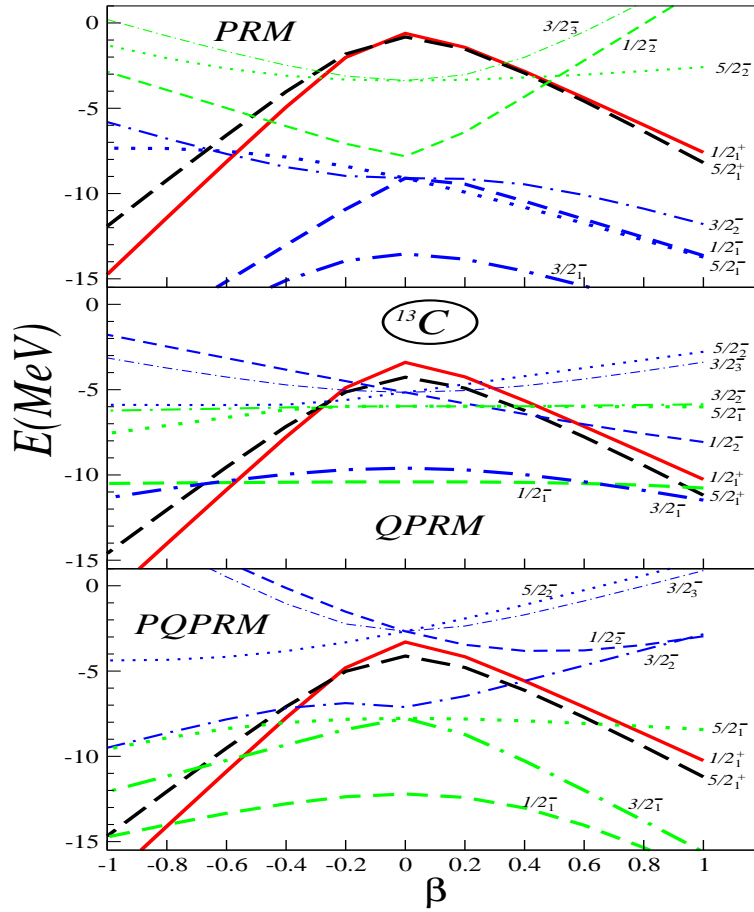


FIG. 4: (Color online) Calculated levels for  $^{13}\text{C}$  as functions of the  $\beta$  value for  $^{12}\text{C}$ , within the PRM, QPRM and PQPRM models.

The vibrational analog of the QPRM, *i.e.*, the quasiparticle-vibrator coupling model (QPVM) has been introduced in Refs. [27, 28, 38]. Note also that when only the collective state  $2^+$  is considered, and the  $2^+ - 2^+$  coupling is neglected, the QPRM and QPVM formally yield the same result, except that the negative value of the deformation parameter  $\beta$  does not have any physical meaning in the vibrational case. The same statement is valid for the projected version of the QPVM, *i.e.*, for the PQPVM.

The s.p.e., used in the previous section, and shown in Table II, already include the collective degrees, by the way they were derived from the experimental data. Therefore they can not be used in the core-particle models. Thus, we have to use here the bare main field s.p.e., which are obtained from a Wood-Saxon potential with standard parametrisation [52]. The resulting neutron s.p.e.  $e_j$  for  $^{13}\text{C}$  and  $^{11}\text{Be}$  are shown in Table III, together with the corresponding quasiparticle BCS and PBGS energies  $E_j^{(+)}$ . As the single-particle space here is smaller than the one used in the previous section, we employ now a somewhat larger pairing strength.

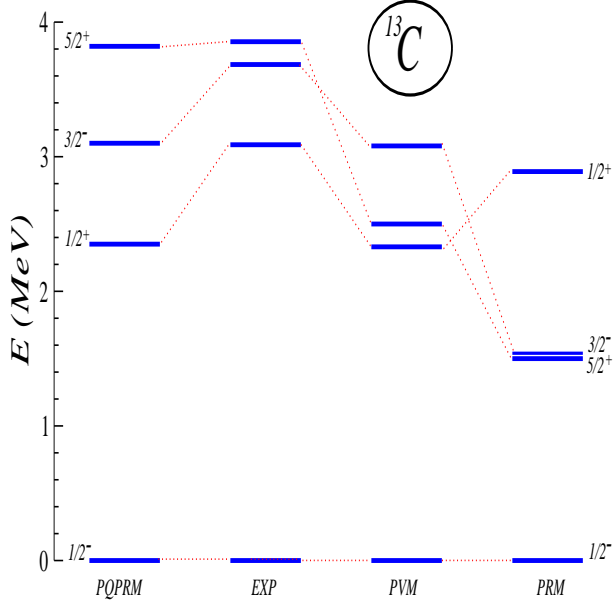


FIG. 5: (Color online) The low-energy spectra in  $^{13}\text{C}$  within the PQPRM for  $\beta = -0.6$ , compared with the experimental levels (EXP) and the PVM [16] and PRM [19] calculations.

Calculated low-lying levels for  $^{13}\text{C}$  as functions of the  $\beta$  value for  $^{12}\text{C}$ , within the PRM, QPRM and PQPRM models are shown in Fig. 4. Let us first note that, in order to simulate the Pauli principle, the lowest states  $I^\pi = 3/2_1^-, 1/2_1^-, 3/2_2^-$  and  $5/2_2^-$ , based on the unperturbed configurations  $|1p_{3/2}, 0^+\rangle$  and  $|1p_{3/2}, 2^+\rangle$ , are frequently just ignored within the PRM [16, 17, 18, 19]. We are considering them, however, in order to make the comparison with the other two models, where these states are physically meaningful. Let us also note that in the PRM the state  $I^\pi = 1/2_2^-$ , build up on  $|1p_{1/2}, 0^+\rangle$ , is considered to be the ground state. Esbensen *et al.* [20], on the other hand, explicitly state that the negative parity states cannot be described reliably in the weak coupling limit because they have a complicate structure due to the importance of the pairing correlations.

The measured quadrupole moment of the core  $^{12}\text{C}$  is  $Q_0 = -(22 \pm 10) \text{ e fm}^2$  [53], suggesting an oblate shape. This gives a quite large quadrupole deformation ( $\beta \cong -0.6$ ). As can be seen from Fig. 4, only the PQPRM reproduces satisfactorily the experimental energy ordering of the lowest four levels in  $^{13}\text{C}$  with this value of  $\beta$ . In Fig. 5 we confront the PQPRM energies for this  $\beta$  of the lowest  $1/2^-, 3/2^-, 1/2^+$  and  $5/2^+$  levels in  $^{13}\text{C}$  with the experimental data, and the PVM [16] and PRM [19] calculations.

It should be noted that the PRM and QPRM are unable to account for the  $^{13}\text{C}$  energy

spectra for any value of the deformation parameter, neither positive nor negative. In the first case, and even when the levels based on the configurations  $|1p_{3/2}, 0^+\rangle$  and  $|1p_{3/2}, 2^+\rangle$  are omitted, a low lying  $5/2^-$  state, arising from the unperturbed  $|1p_{1/2}, 2^+\rangle$  level, shows up, which is not observed experimentally. On the other hand, in the second case, the particle-core coupling never removes the degeneracy between the states  $1/2_1^-$  and  $3/2_1^-$ .

The resulting PRM, QPRM and PQPRM wave functions for the  $1/2^-$  and  $3/2^-$  states, with  $\beta = -0.6$ , are:

$$|1/2^-\rangle = \begin{pmatrix} 0.849 \\ 0.997 \\ 0.961 \end{pmatrix} |1p_{1/2}; 0^+\rangle + \begin{pmatrix} 0.528 \\ 0.076 \\ 0.277 \end{pmatrix} |1p_{3/2}; 2^+\rangle, \quad (3.17)$$

and

$$|3/2^-\rangle = \begin{pmatrix} -0.162 \\ 0.935 \\ -0.650 \end{pmatrix} |1p_{3/2}; 0^+\rangle + \begin{pmatrix} 0.332 \\ 0.350 \\ 0.025 \end{pmatrix} |1p_{3/2}; 2^+\rangle + \begin{pmatrix} 0.929 \\ -0.052 \\ 0.759 \end{pmatrix} |1p_{1/2}; 2^+\rangle. \quad (3.18)$$

As mentioned before, within QPRM and PQPRM these states are the lowest ones, but in the PRM they correspond, respectively, to the second  $1/2^-$  level and to the third  $3/2^-$  level. It is worth noting that the pairing makes the wave functions of these two states less collective. In the previous PRM evaluation of the negative parity states done by Nunes *et al.* [18], 32% of the lowest  $1/2^-$  state consists of an  $1p_{1/2}$  single-particle state coupled to the  $0^+$  core, while the remaining 67% comes from a  $1p_{3/2}$  state coupled to the  $2^+$  core state. In contrast, we get that the ground state in  $^{13}\text{C}$  is basically ( $\cong 92\%$ ) the single-particle  $1p_{1/2}$  state. Their wave function for the lowest  $3/2^-$  is build up from states  $|1p_{3/2}; 0^+\rangle$ ,  $|1p_{3/2}; 2^+\rangle$  and  $|1p_{1/2}; 2^+\rangle$  in proportions of 14.1%, 23.9% and 62%, respectively. Therefore, as seen from (3.18), it is also quite different from our  $3/2^-$  wave function.

The wave function (3.17) can be compared with the one obtained by Vinh Mau [16] in the PVM,

$$|1/2^-\rangle = 0.791|1p_{1/2}; 0^+\rangle + 0.602|1p_{3/2}; 2^+\rangle + \dots \quad (3.19)$$

It is quite similar to our PRM wave function, but significantly different from the PQPRM result. The lowest  $3/2^-$  is described Ref. [16] as the  $|1p_{3/2}^{-1}\rangle$  neutron-hole state coupled to the  $^{14}\text{C}$  core, but its wave function is not shown in the paper. Note that within such a coupling

scheme, and in order to be consistent, in (3.19) one should have the ket  $|1p_{3/2}^{-1}; 2^+(^{14}\text{C})\rangle$ , instead of the ket  $|1p_{3/2}; 2^+(^{12}\text{C})\rangle$ . <sup>1</sup>

The PRM, QPRM and PQPRM wave functions for the  $1/2_1^+$  and  $5/2_1^+$  states, with  $\beta = -0.6$ , are:

$$|1/2_1^+\rangle = \begin{pmatrix} 0.684 \\ 0.672 \\ 0.671 \end{pmatrix} |2s_{1/2}; 0^+\rangle + \begin{pmatrix} 0.730 \\ 0.741 \\ 0.741 \end{pmatrix} |1d_{5/2}; 2^+\rangle, \quad (3.20)$$

and

$$|5/2_1^+\rangle = \begin{pmatrix} 0.737 \\ 0.752 \\ 0.749 \end{pmatrix} |1d_{5/2}; 0^+\rangle + \begin{pmatrix} -0.471 \\ -0.469 \\ -0.471 \end{pmatrix} |1d_{5/2}; 2^+\rangle + \begin{pmatrix} 0.485 \\ 0.463 \\ 0.466 \end{pmatrix} |2s_{1/2}; 2^+\rangle, \quad (3.21)$$

Thus, all three models used here yield similar results for the positive parity state.

We find about 55% of the  $1/2_1^+$  state consists of the  $1d_{5/2}$  single-particle state coupled to the  $2^+$  excited core state, while the remaining 45% comes from the  $2s_{1/2}$  single-particle coupled to the  $0^+$  ground state of the core. Contrarily, in the previous particle-core coupling calculations [16, 19, 20] it was found that this state is basically ( $\geq 90\%$ ) of single-particle nature.

For the  $5/2_1^+$  we find that its wave function is build up  $\cong 55\%$  from the  $1d_{5/2}$  state coupled to the  $0^+$  ground state of the core and  $\cong 22\%$  from the  $1d_{5/2}$  state coupled to the  $0^+$  ground state of the core and  $\cong 22\%$  from the  $2s_{1/2}$  state coupled to the  $2^+$ . The wave function is also quite different, from those derived in similar studies [16, 19, 20], were the just mentioned percentages are, respectively: 75, 9, and 3 in Ref. [16], 69, 29, and 0.3 in Ref. [18] and 80, 18, and 2 in Ref. [20]. Therefore, our  $5/2_1^+$  wave function is significantly more collective because of the coupling of the  $2s_{1/2}$  single-particle state to the  $2^+$  core state.

The reaction spectroscopic factors for pickup on the  $^{13}\text{C}$  target and for stripping on the  $^{12}\text{C}$  target, evaluated with the wave functions (3.17), (3.18), (3.20) and (3.21), are shown in Table IV. In the same table are also listed the results of previous PRM [19, 20], and shell model [55] studies, as well as the experimental results [50, 51, 56], which are accounted for quite well within the present PQPRM calculations.

---

<sup>1</sup> The description of an A-mass odd nucleus as a particle coupled to the A-1 core plus a hole state coupled to the A+1 core have been done in the past [54]

TABLE IV: Reaction spectroscopic factors for pickup on the  $^{13}\text{C}$  target and for stripping on the  $^{12}\text{C}$  target. The results obtained with the wave functions (3.17), (3.18), (3.20) and (3.21), as well as the previous PRM [19, 20], and shell model [55], are shown and confronted with experimental data [50, 51, 56].

State	Theory						Experiment		
	PRM	QPRM	PQPRM	Ref. [19]	Ref. [20]	Ref. [55]	Ref. [56]	Ref. [51]	Ref. [50]
$1/2^-$	0.72	0.69	0.53	0.32		0.61	$0.58 \pm 0.15$	0.77	$0.61 \pm 0.09$
$1/2^+$	0.47	0.44	0.44	0.90	0.95		$0.36 \pm 0.02$	0.65	
$3/2^-$	0.03	0.17	0.10			0.19		0.14	
$5/2^+$	0.54	0.55	0.55		0.80			0.58	

In Fig. 6 we show the PRM, QPRM and PQPRM results of our study of the low-lying states in  $^{11}\text{Be}$  as a function of deformation. All what has been pointed out in commenting the  $^{13}\text{C}$  nucleus in the PRM, regarding the Pauli principle, the unperturbed configurations  $|1p_{3/2}, 0^+\rangle$  and  $|1p_{3/2}, 2^+\rangle$ , and the negative parity states, is also pertinent here. On the other hand, when comparing our PRM results with the work of Esbensen *et al.* [20] one sees that their deformation dependence of the levels  $1/2^+$  and  $5/2^+$  gets flatter than ours for strong deformations. The reason for that is simple and comes from the fact that they use a volume factor in the calculation, given by [20, (3)], to preserve the volume of the nucleus. This actually means that their interaction radius is smaller for higher deformations and this results in the flattening of the curves. Said that, it should be noted that our PRM curves for the states  $1/2_1^+$  and  $1/2_2^-$  are very much like those in [19, Fig. 2]. The main difference is that in our case the crossings between the positive and negative  $1/2$  states occur at a significantly smaller value of  $\beta$ , which means that our radial matrix elements  $\langle j'|k|j\rangle$  are quite larger than theirs.

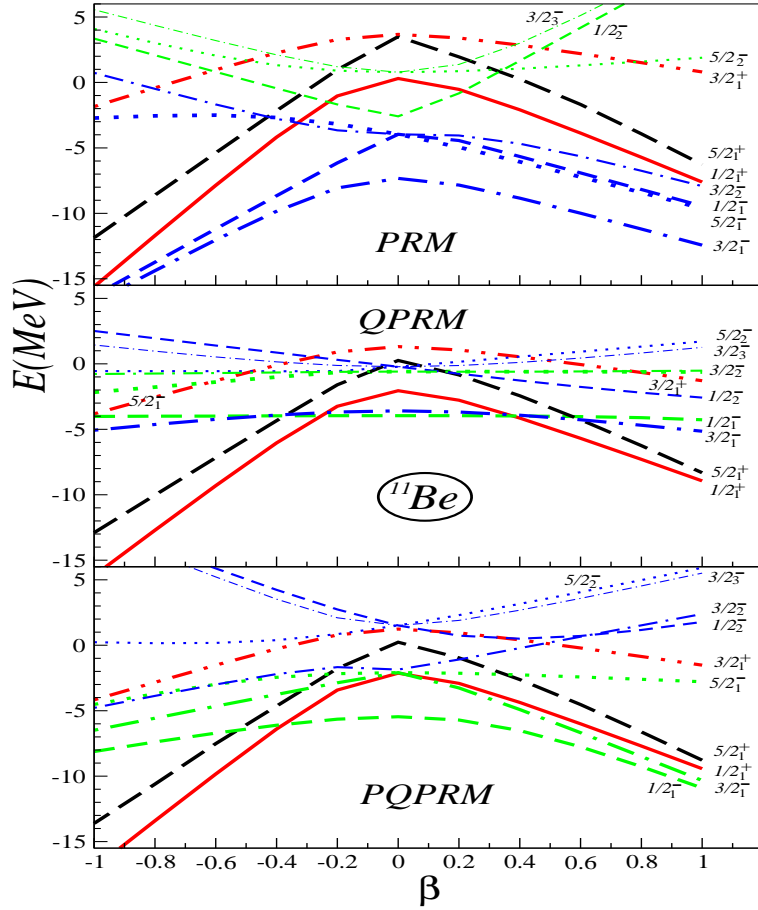


FIG. 6: (Color online) Calculated levels for  $^{11}\text{Be}$  as functions of the  $\beta$  value for  $^{10}\text{Be}$ , within the PRM, QPRM and PQPRM models.

Both PRM calculations performed so far [19, 20] were done with a positive value of  $\beta$ , *i.e.*, a prolate deformation has been assumed for the  $^{10}\text{Be}$  nucleus. However, there is no firm experimental evidence that it is so. Worse even, we neither know whether  $^{10}\text{Be}$  behaves as a rotator or as a vibrator. From its energy spectra, with the first and second  $2^+$  at energies  $E_{2_1^+} = 3.37$  MeV and  $E_{2_2^+} = 5.96$  MeV (*i.e.*,  $E_{2_2^+} \cong 2E_{2_1^+}$ ), one can conclude that it is more likely a vibrator. In fact, Esbensen *et al.* [20] have noted that for the positive parity spectra in  $^{11}\text{Be}$  a better agreement with data is obtained after reducing (in 34%) the  $2^+ - 2^+$  coupling strength. On the other hand, Vinh Mau [16] and Coló *et al.* [17] use straightforwardly the PVM.

The most recent study of quadrupole deformation of  $^{10}\text{Be}$  has been done through the proton inelastic scattering [57], and the values for  $\beta$ , extracted from the measured deformation lengths  $\delta = \beta R = \beta r_0 A^{1/3}$ , are:  $\beta = 0.593(56)$  and  $\beta = 0.692(65)$ . From a careful scrutinising of the energy levels in Fig. 6, one can easily convince oneself that, none of our particle-rotor coupling calculations is able to reproduce the experimentally observed spin

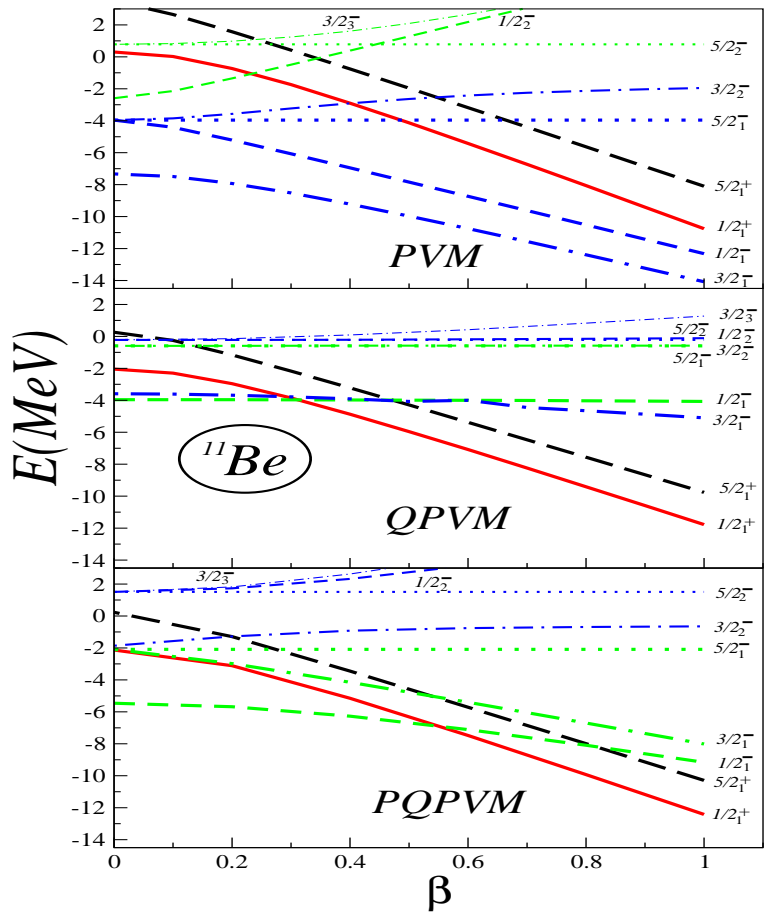


FIG. 7: (Color online) Calculated levels for  $^{11}\text{Be}$  as functions of the  $\beta$  value for  $^{10}\text{Be}$ , within the PVM, QPVM and PQPVM models.

sequence  $1/2^+ - 1/2^- - 5/2^+$  in  $^{11}\text{Be}$ , for such a value of  $\beta$  neither positive nor negative. In view of this it does not make much sense to discuss the wave functions within the PRM, QPRM and PQPRM approximations.

Because of all said above, we decided to substitute the rotor by a harmonic vibrator in the description of the low-lying  $^{11}\text{Be}$  levels. The results are shown in Fig. 7. The PVM (upper panel) exhibits the same features as the PRM regarding the Pauli principle. Therefore the lowest four negative parity states, have to be discarded again. However, even doing so it is not possible to obtain the desired theoretical results. On the other hand, from the QPVM energy spectra (middle panel) one sees that the particle-vibrator coupling, same as the particle-rotor coupling, is unable to remove the degeneracy between the states  $1/2_1^-$  and  $3/2_1^-$ . Once more, as seen from the PQPRM results (lower panel), this is only achieved through the number projection procedure. Note that both  $1/2_1^+$  and  $1/2_1^-$  levels go down when  $\beta$  is increased and that their crossing happens close to the experimental value for the deformation parameter ( $\beta \cong 0.6$ ). Thus, the spin inversion mechanism is quite different here

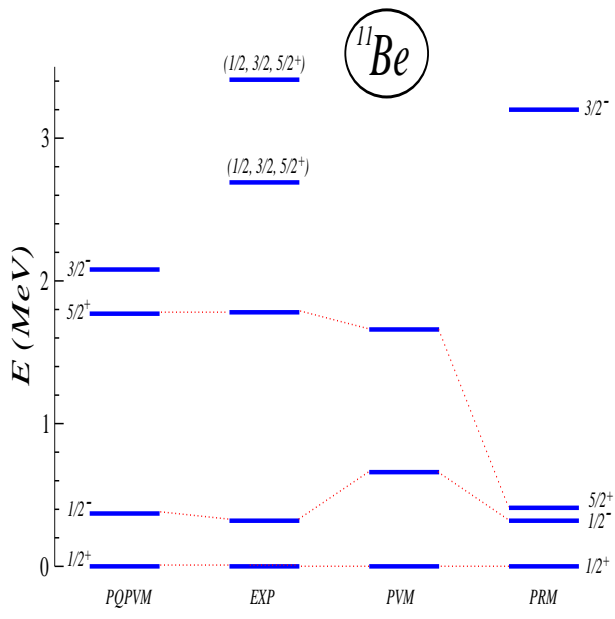


FIG. 8: (Color online) The low-energy spectra in  $^{11}\text{Be}$  within the PQPVM for  $\beta = 0.6$ , compared with the experimental levels (EXP) and the PVM [16] and PRM [19] calculations.

than in the PRM and PVM cases, where the  $1/2_1^-$  state is pushed up while the  $1/2_1^+$  state is pushed down [16, 19].

As shown in Fig. 8 all three lowest states in  $^{11}\text{Be}$  are satisfactorily reproduced within the PQPVM for  $\beta = 0.6$ . For the sake of comparison in the same figure are also presented the results of the PVM [16] and PRM [19] calculations.

The corresponding PVM, QPVM and PQPVM wave functions for negative parity states are:

$$|1/2^-\rangle = \begin{pmatrix} 0.750 \\ 0.995 \\ 0.916 \end{pmatrix} |1p_{1/2}; 0^+\rangle + \begin{pmatrix} -0.631 \\ -0.103 \\ -0.401 \end{pmatrix} |1p_{3/2}; 2^+\rangle, \quad (3.22)$$

and

$$|3/2^-\rangle = \begin{pmatrix} 0.428 \\ 0.927 \\ 0.735 \end{pmatrix} |1p_{3/2}; 0^+\rangle + \begin{pmatrix} -0.247 \\ -0.368 \\ -0.331 \end{pmatrix} |1p_{3/2}; 2^+\rangle + \begin{pmatrix} 0.870 \\ 0.070 \\ 0.592 \end{pmatrix} |1p_{1/2}; 2^+\rangle. \quad (3.23)$$

The PVM wave function (3.19) for the  $1/2_1^-$  state, obtained by Vinh Mau [16] is quite similar to the one we get within the same model. Note that the pairing makes this state to be less collective.

All three models (PVM, QPVM and PQPVM) yields similar results for the positive parity

wave functions. Namely:

$$|1/2_1^+\rangle = \begin{pmatrix} 0.826 \\ 0.825 \\ 0.821 \end{pmatrix} |2s_{1/2}; 0^+\rangle + \begin{pmatrix} -0.564 \\ -0.565 \\ -0.571 \end{pmatrix} |1d_{5/2}; 2^+\rangle, \quad (3.24)$$

and

$$|5/2_1^+\rangle = \begin{pmatrix} 0.740 \\ 0.760 \\ 0.758 \end{pmatrix} |1d_{5/2}; 0^+\rangle + \begin{pmatrix} 0.422 \\ 0.375 \\ 0.437 \end{pmatrix} |1d_{5/2}; 2^+\rangle + \begin{pmatrix} -0.523 \\ -0.486 \\ -0.485 \end{pmatrix} |2s_{1/2}; 2^+\rangle. \quad (3.25)$$

They can be confronted with

$$\begin{aligned} |1/2^+\rangle &= 0.964|2s_{1/2}; 0^+\rangle + 0.267|1d_{5/2}; 2^+\rangle, \\ |5/2^+\rangle &= 0.896|1d_{5/2}; 0^+\rangle + 0.352|1d_{5/2}; 2^+\rangle + 0.269|2s_{1/2}; 0^+\rangle, \end{aligned} \quad (3.26)$$

which were derived within the PVM by Vinh Mau [16]. Note that, at variance with what happens with negative parity states, the wave functions (3.25) and (3.26) are more collective than the those from Ref. [16]. We also note that our wave function for the  $1/2_1^+$  state is

TABLE V: Reaction spectroscopic factors for pickup on the  $^{11}\text{Be}$  target and for stripping on the  $^{10}\text{Be}$  target. The results obtained with the wave functions (3.22), (3.23), (3.24) and (3.25), as well as the previous PRM [19, 20], and shell model [55], are shown and confronted with experimental data [8, 58, 59].

State	Theory						Experiment		
	PVM	QPVM	PQPVM	Ref. [19]	Ref. [20]	Ref. [55]	Ref. [58]	Ref. [59]	Ref. [8]
$1/2^+$	0.68	0.62	0.64	0.78	0.87		$0.73 \pm 0.06$	0.77	$0.53 \pm 0.13$
$1/2^-$	0.56	0.63	0.49	0.87		0.60	$0.63 \pm 0.15$	0.96	$0.45 \pm 0.12$
$5/2^+$	0.54	0.56	0.56					0.50	
$3/2^-$	0.18	0.25	0.15			0.17			

similar to that obtained in the variational shell model (VSM) calculation of Otsuka *et al.* Ref. [60], which yields

$$|1/2^+\rangle = 0.74|2s_{1/2}; 0^+\rangle + 0.63|1d_{5/2}; 2^+\rangle + \dots \quad (3.27)$$

The reaction spectroscopic factors for pickup on the  $^{11}\text{Be}$  target and for stripping on the  $^{10}\text{Be}$  target, evaluated with the wave functions (3.22), (3.23), (3.24) and (3.25), are shown in Table V. From there we can read the differences with the previous PRM results for the  $1/2_1^+$  state [19, 20], and the similarity with the shell model calculation for the negative parity states [55]. In the same table we also list the experimental data [8, 58, 59] for the levels  $1/2_1^+, 1/2_1^-$  and  $5/2_1^+$ , which are reproduced quite well by the PQPVM.

#### IV. SUMMARY AND CONCLUSIONS

In this work we study the interplay between the pairing correlations and collective degrees of freedom in the structure of neutron-rich carbon nuclei and of the  $^{11}\text{Be}$  nucleus. The pairing effects were taken into account by using both the simple BCS method and the particle number projected BCS (PBCS) formalism.

Our work was divided into two main stages. First, we apply pure BCS and PBCS models to describe heavy carbon isotopes. We use the single-particle energies and pairing strengths of Ref. [23] fixed so that the experimental binding energies of  $^{11}\text{C}$  and  $^{13}\text{C}$ , together with the  $^{13}\text{C}$  energy spectra, are reproduced by the calculations. With these parameters we evaluate next the low-lying states in  $^{15}\text{C}$ ,  $^{17}\text{C}$  and  $^{19}\text{C}$ , by augmenting correspondingly the number of neutrons only. We found that proceeding in this way both models are capable to explain fairly well the decrease of the binding energies in going from  $^{13}\text{C}$  to  $^{19}\text{C}$ . The PBCS model reproduces as well the experimentally observed spin ordering  $1/2^+, 5/2^+, 3/2^+$  of the lowest three states in  $^{15}\text{C}$  and the energy of the first  $3/2^-$  state. Although the pure pairing models cannot describe the  $3/2^+$  ground state in  $^{17}\text{C}$ , the PBCS correctly predicts the first two excited states in this nucleus to be  $1/2^+$  and  $5/2^+$ . Finally, the spin and the parity of the ground state  $1/2^+$  in  $^{19}\text{C}$  is correctly reproduced within BCS and PBCS models. The recently observed two excited states  $3/2^+$  and  $5/2^+$  in this nucleus at 197(6) keV and 268(8) keV, respectively, are also obtained theoretically but in an inverted order.

We have calculated the one-particle reaction spectroscopic factors for the lowest  $1/2^-, 3/2^-, 1/2^+$  and  $5/2^+$  states for all four odd-mass C isotopes obtaining quite similar results within the two pairing models. In  $^{13}\text{C}$  the results of calculation agree with the experimental data for the ground state, but they fail to reproduce the experimental spectroscopic factors for excited states in this nucleus. For heavier carbon isotopes the agreement with the

experimental data is better. This implies that the low-lying states in  $^{15,17,19}\text{C}$  are basically seniority-one states, while the contribution of seniority-three states and the collective effects could be important in  $^{13}\text{C}$ . One should also keep in mind that the ground state in  $^{17}\text{C}$  is very likely build up mainly on the anomalous seniority-three state  $|(1d_{5/2})^3 J^\pi = 3/2^+\rangle$ . Briefly, the just summarised results clearly indicate that the pairing interaction plays the main role in the nuclear structure of heavy carbon isotopes, accounting for their basic feature such as: a) small binding energies, b) spin-parity ordering of the low-lying states, and c) systematic decrease in the binding when one goes from  $^{13}\text{C}$  to  $^{19}\text{C}$ . Therefore, it has to be taken into account in any theoretical calculation that aspire to be quantitatively realistic.

On the next stage we included the collective degrees of freedom within the framework of the weak-coupling model and applied it to describe  $^{13}\text{C}$  and  $^{11}\text{Be}$ . Our main objective here was to analyse how the short range pairing correlation modify the core-particle coupling mechanism, and consequently the energy spectra in this nuclei. As far as we know such a study has not been done so far, at least not in systematic way. It is worthwhile to stress once more that the Pauli principle, which is currently omitted in the simple particle-rotor and particle-vibrator coupling models, is brought up into the play by the pairing.

In the present work the single-particle energies were taken from the standard parametrisation for the Wood-Saxon potential and the coupling matrix elements were calculated using the wave functions of the harmonic oscillator. This could be a rather crude approach for a weakly bound nucleus such as  $^{11}\text{Be}$ . Nevertheless, we feel that it is sufficiently good to reveal the importance of the Pauli principle.

We found that only PQPRM reproduces satisfactorily the experimental ordering of the lowest four levels in  $^{13}\text{C}$  with the correct value of deformation  $\beta = -0.6$ . Neither the PRM nor the QPRM could accomplish this. The inclusion of pairing strongly reduces the coupling with the excited states of the core for the negative parity states  $1/2^-$  and  $1/3^-$ , compared to earlier works. In fact, we obtain the ground state of  $^{13}\text{C}$  to be basically the single-particle  $1p_{1/2}$  state. Contrarily, our positive parity states  $1/2^+$  and  $5/2^+$  are more collective when compared to results of the previous works. Moreover, the spectroscopic factors are accounted quite well within the present PQPRM calculations.

Similar calculations were done for one-neutron halo nucleus  $^{11}\text{Be}$ . It is found that the more likely structure of the core,  $^{10}\text{Be}$ , required to reproduce the lowest three states in  $^{11}\text{Be}$ , is that of a vibrator. Moreover, we feel that the appropriate model for the experimental value

of the vibrational length,  $\beta = 0.6$ , is again the PQPVM. As before, we found that inclusion of pairing makes the negative-parity states less collective and positive parity states more collective compared to earlier works. Also, the spectroscopic factors are reproduced quite well by the PQPVM.

In summary, the inclusion of the pairing interaction and of the concomitant Pauli principle is imperative not only in the case of heavy odd-mass carbon isotopes but also in the core-coupling models of  $^{13}\text{C}$  and  $^{11}\text{Be}$ . The important role played by the particle number conservation in these relatively light and/or exotic nuclei has been confirmed as well.

### Acknowledgments

Authors would like to acknowledge the partial support of Brazilian agencies FAPESP and CNPq.

---

- [1] M. Bender, P.H. Heenen, and P.G Reinhard, Rev. Mod. Phys. **75**, 121 (2003).
- [2] J. Dobaczewski, and W. Nazarewicz, Prog. Theor. Phys. Suppl. **146**, 70 (2003).
- [3] B. Jonson, Phys. Rep. **389**, 1 (2004).
- [4] A.S. Jensen, K.Riisager, D.V. Fedorov, and E. Garrido, Rev. Mod. Phys. **76**, 215 (2004).
- [5] J. Dobaczewski, I. Hamamoto, W. Nazarewicz, and J.A. Sheikh, Phys. Rev. Lett. **72**, 981 (1994).
- [6] J. Dobaczewski, W. Nazarewicz, T.R. Werner, J.F. Berger, C.R. Chinn, and J. Dechargé, Phys. Rev. C **53**, 2809 (1996).
- [7] H. Iwasaki, T. Motobayashi, H. Akiyoshi, Y. Ando, N. Fukuda, H. Fujiwara, Zs. Flp, K. I. Hahn, Y. Higurashi, M. Hirai, I. Hisanaga, N. Iwasa, T. Kijima, A. Mengoni, T. Minemura, T. Nakamura, M. Notani, S. Ozawa, H. Sagawa, H. Sakurai, S. Shimoura, S. Takeuchi, T. Teranishi, Y. Yanagisawa, and M. Ishihara , Eur. Phys. J. A **13**, 55 (2000).
- [8] A. Navin, D.W. Anthony, T. Aumann, T. Baumann, D. Bazin, Y. Blumenfeld, B.A. Brown, T. Glasmacher, P. G. Hansen, R.W. Ibbotson, P.A. Lofy, V. Maddalena, K. Miller, T. Nakamura, B. V. Pritychenko, B.M. Sherrill, E. Spears, M. Steiner, J.A. Tostevin, J. Yurkon, and A. Wagner, Phys. Rev. Lett. **85**, 266 (2000).

- [9] A. Ozawa, T. Kobayashi, T. Suzuki, K. Yoshida, and I. Tanihata, Phys. Rev. Lett **84**, 5493 (2000).
- [10] T. Otsuka, R. Fujimoto, Y. Utsuno, B.A. Brown, M. Honma, and T. Mizusaki, Phys. Rev. Lett. **87**, 082502 (2001).
- [11] R. Kanungo, I. Tanihata, and A. Ozawa, Phys. Lett. **B528**, 58 (2002).
- [12] I. Hamamoto and B.R. Mottelson, Phys. Rev. C **68**, 034312 (2003).
- [13] I. Hamamoto and B.R. Mottelson, Phys. Rev. C **69**, 064302 (2004).
- [14] K. Bennaceur, J. Dobaczewski, and M. Ploszajczak, Phys. Lett. **B496**, 154 (2000).
- [15] I. Hamamoto, Phys. Rev. C **71**, 037302 (2005).
- [16] N. Vinh Mau, Nucl. Phys. **A592**, 33 (1995).
- [17] G. Coló, Toshio Suzuki, and H. Sagawa, Nucl. Phys. **A695**, 167 (2001).
- [18] F.M. Nunes, *Core Excitation in Few Body Systems: Application to halo nuclei*, (PhD thesis, University of Surrey, 1995, unpublished).
- [19] F.M. Nunes, I.J. Thompson, and R.C. Johnson, Nucl. Phys. **A596**, 171 (1996).
- [20] H. Esbensen, B.A. Brown, and H. Sagawa, Phys. Rev. C **51**, 1274 (1995).
- [21] D. Ridikas, M.H. Smedberg, J.S. Vaagen and M.V. Zhukov, Nucl. Phys. **A628**, 363 (1998).
- [22] H. Sagawa, B.A. Brown, and H. Esbensen, Phys. Lett. **B309**, 1 (1993).
- [23] F. Krmpotić, A. Mariano, and A. Samana, Phys. Lett. **B541**, 298 (2002); Phys. Rev. C **71**, 44319 (2005).
- [24] P.L. Ottaviani, and M. Savoia, Phys. Rev. **178**, 1594 (1969); Phys. Rev. **188**, 1306 (1969).
- [25] L. S. Kisslinger and R. A. Sorensen, Rev. Mod. Phys. **35**, 853 (1963).
- [26] W. Scholz and F.B. Malik, Phys. Rev. **176**, 1355 (1968).
- [27] K.W.C. Steward, B. Castel, and B.P. Singh, Phys. Rev. C **4**, 2131 (1971).
- [28] B. Barman Roy, and D.C. Choudhury, Phys. Rev. C **12**, 323 (1975).
- [29] B.L. Cohen and R.E. Price, Phys. Rev. **121**, 1441 (1960).
- [30] P.J. Siemens and A.S. Jensen, *Elements of Nuclei: Many Body Physics with the Strong Interaction* (Addison-Wesley Publishing Company Inc., Redwood City, California, 1987).
- [31] F. Ajzenberg-Selove, Nucl. Phys. **A433**, 1 (1985) ; TUNL Nuclear Data Evaluation Project, available WWW: <http://www.tunl.duke.edu/nucldata/>
- [32] Z. Elekes, Z. Dombradi, R. Kanungo, H. Baba, Z. Fulop, J. Gibelin, A. Horvath, E. Ideguchi, Y. Ichikawa, N. Iwasa, H. Iwasaki, S. Kanno, S. Kawai, Y. Kondo, T. Motobayashi, M. Notani,

T. Ohnishi, A. Ozawa, H. Sakurai, S. Shimoura, E. Takeshita, S. Takeuchi, I. Tanihata, Y. Togano, C. Wu, Y. Yamaguchi, Y. Yanagisawa, A. Yoshida, and K. Yoshida, Phys. Lett. **B614**, 174 (2005).

[33] F. Cappuzzello, S. E. A. Orrigo, A. Cunsolo, H. Lenske, M. C. Allia, D. Beaumel, S. Fortier, A. Foti, A. Lazzaro, C. Nociforo and J. S. Winfield, Europhys. Lett. **65** (6), 766 (2004).

[34] G. Thiamova, N. Itagaki, T. Otsuka, and K. Ikeda, Eur. Phys. J. **A22**, 461 (2004).

[35] D.R. Tilley, H.R. Weller and C.M. Cheves, Nucl. Phys. **A564**, 1 (1993).

[36] E.K. Warburton and B.A. Brown, Phys. Rev. C **46**, 923 (2000).

[37] V. Maddalena, T. Aumann, D. Bazin, B. A. Brown, J. A. Caggiano, B. Davids, T. Glasmacher, P. G. Hansen, R. W. Ibbotson, A. Navin, B. V. Pritychenko, H. Scheit, B. M. Sherrill, M. Steiner, J. A. Tostevin, and J. Yurkon, Phys. Rev. C **63**, 024613 (2001).

[38] A. Bohr and B.R. Mottelson, *Nuclear Structure*, vol.II, (W.A. Benjamin, Inc. 1975).

[39] D. Kurath, Phys. Rev. **80**, 98 (1950).

[40] V. Paar, Nucl. Phys. **A211**, 29 (1973)

[41] O. Civitarese and F. Krmpotić, Nucl. Phys. **A229**, 133 (1973).

[42] D. Bazin, B. A. Brown, J. Brown, M. Fauerbach, M. Hellström, S. E. Hirzebruch, J. H. Kelley, R. A. Kryger, D. J. Morrissey, R. Pfaff, C. F. Powell, B. M. Sherrill, and M. Thoennessen, Phys. Rev. Lett. **74**, 3569 (1995).

[43] T. Nakamura, N. Fukuda, T. Kobayashi, N. Aoi, H. Iwasaki, T. Kubo, A. Mengoni, M. Notani, H. Otsu, H. Sakurai, S. Shimoura, T. Teranishi, Y. X. Watanabe, K. Yoneda, and M. Ishihara, Phys. Rev. Lett. **83**, 1112 (1999).

[44] D. Cortina-Gil, T. Baumann, H. Geissel, H. Lenske, K. Sümmerer, L. Axelsson, U. Bergmann, M.J.G. Borge, L.M. Fraile, M. Hellström, M. Ivanov, N. Iwasa, R. Janik, B. Jonson, K. Markenroth, G. Münzenberg, F. Nickel, T. Nilsson, A. Ozawa, K. Riisager, G. Schrieder, W. Schwab, H. Simon, C. Scheidenberger, B. Sitar, T. Suzuki and M. Winkler, Eur. Phys. J. **A10**, 49 (2001).

[45] G. Audi and A.H. Wapstra, Nucl. Phys. **A565**, 1 (1993); G. Audi, O. Besillón, J. Blashot and A.H. Wapstra, *ibid.* **A624**, 1 (1997).

[46] G. Audi, A.H. Wapstra and C. Thibault, Nucl. Phys. **A729**, 337 (2003).

[47] M.B. Tsang, Jenny Lee, and W.G. Lynch, <http://arXiv.org/abs/nucl-ex/0506016>.

[48] B. A. Brown, Prog. Part. Nucl. Phys. **47**, 517 (2001).

[49] D. Bazin, W. Benenson, B.A. Brown, J. Brown, B. Davids, M. Fauerbach, P.G. Hansen, P. Mantica, D.J. Morrissey, C.F. Powell, B.M. Sherrill, and M. Steiner, Phys. Rev. C **57**, 2156 (1998).

[50] X.D. Liu, M.A. Famiano, W.G. Lynch, M. B. Tsang, and J. A. Tostevin, Phys. Rev. C **69**, 064313 (2004).

[51] H. Ohnuma, N. Hoshino, O. Mikoshiba, K. Raywood, A. Sakaguchi, G.G. Shute, B.M. Spicer, M.H. Tanaka, M. Tanifuji, T. Terasawa, and M. Yasue, Nuc. Phys. **A448**, 205 (1985).

[52] A. Bohr and B.R. Mottelson, *Nuclear Structure*, vol.I, (W.A. Benjamin, Inc. 1969).

[53] W. J. Vermeer, M. T. Esat, J. A. Kuehner, and R. H. SpearA. M. Baxter and S. Hinds, Phys. Lett. **B122**, 23 (1983).

[54] S.M. Abecasis, O. Civitarese and F. Krmpotić, Phys. Rev. C **9**, 2320 (1974).

[55] B. Cohen and D. Kurath, Nuc. Phys. **A101**, 1 (1967).

[56] C.A. Pearson, J.M. Covar, D. Zissermann, T.G. Miller, F.P. Gibson, R. Haglund, W. Morrison and G. Westley, Nuc. Phys. **A191**, 1 (1972).

[57] H. Iwasaki, T. Motobayashi, H. Akiyoshi, Y. Ando, N. Fukuda, H. Fujiwara, Zs. Flp, K. I. Hahn, Y. Higurashi, M. Hirai, I. Hisanaga, N. Iwasa, T. Kijima, T. Minemura, T. Nakamura, M. Notani, S. Ozawa, H. Sakurai, S. Shimoura, S. Takeuchi, T. Teranishi, Y. Yanagisawa and M. Ishiharaa, Phys. Lett. **B481**, 7 (2000).

[58] D.L. Auton, Nuc. Phys. **A157**, 305 (1970).

[59] B. Zwieglinsky, W. Benenson and R.G.H. Robertson, Nuc. Phys. **A315**, 124 (1979).

[60] T. Otsuka, N. Fukunishi and H. Sagawa, Phys. Rev. Lett. **70**, 1385 (1993).